

Water Transport in 2-Hydroxyethyl Methacrylate Copolymer Irradiated by γ Rays in Air and Related Phenomena*

K. F. CHOU,¹ C. C. HAN,² SANBOH LEE¹

¹ Department of Materials Science, National Tsing Hua University, Hsinchu, Taiwan

² Polymers Division, National Institute of Standards and Technology, Gaithersburg, Maryland 20899

Received 14 April 1999; revised 9 November 1999; accepted 24 November 1999

ABSTRACT: The water transport in 2-hydroxyethyl methacrylate copolymer (HEMA copolymer) irradiated by γ rays in air is investigated. The sorption data of deionized water transport in HEMA copolymer subjected to various dosages of γ -ray irradiation are in excellent agreement with the theoretical model that accounts for case I, case II, and anomalous transport. The diffusion coefficient for case I and the velocity for case II satisfy the Arrhenius equation for all dosage levels. The transport process is exothermic and the equilibrium–swelling ratio satisfies the van't Hoff plot. The studies of the glass transition temperature of the irradiated HEMA copolymer, the pH value of deionized water after irradiation treatment, and the quantitative determination of water structures in the HEMA copolymer hydrogel are helpful in analyzing the irradiation effect on water transport in the HEMA copolymer. The effect of irradiation on the optical properties of the HEMA copolymer is also analyzed. The transmittance of a standard specimen with saturated water is lower than that before the water treatment because of the creation of holes. However, because of the formation of color centers, the color of the copolymer becomes yellow to brown and the UV cutoff wavelength of the HEMA copolymer shifts to the longer wavelength side with increasing irradiation dosage. Some of the color centers can be annihilated after water treatment. The buckled pattern on the outer surface is observed when the HEMA copolymer irradiated by a γ ray in air is immersed in the water. This phenomenon is explained by the inhomogeneous distribution of crosslinking density. © 2000 John Wiley & Sons, Inc. *J Polym Sci B: Polym Phys* 38: 659–671, 2000

Keywords: water transport; 2-hydroxyethyl methacrylate copolymer; γ rays

INTRODUCTION

The 2-hydroxyethyl methacrylate (HEMA) copolymers have been widely studied and employed as biomaterials, including soft contact lenses,^{1,2} kidney dialysis systems,^{3,4} drug delivery systems^{5,6}

and artificial liver support systems.^{7,8} The presence of a hydroxyl group and a carbonyl group on each repeated unit makes the polymers compatible with water, and the hydrophobic α -methyl group and backbone impart hydrolytic stability to the polymers and support the mechanical strength of the polymer matrix.^{9–11} The state and properties of water in crosslinked HEMA gels and their equilibrium swelling behavior have been investigated by many laboratories,^{12–16} but most of the studies have focused on the equilibrium state instead of transients and kinetics of transport properties of the solvent in crosslinked HEMA. In this study we concentrate on the irradiation effect

Correspondence to: S. Lee (E-mail: sblee@mse.nthu.edu.tw)

* The equipment and instruments or materials are identified in this article to adequately specify the experimental details. Such identification does not imply recommendation by the National Institute of Standards and Technology nor does it imply the materials are the best available.

Journal of Polymer Science: Part B: Polymer Physics, Vol. 38, 659–671 (2000)
© 2000 John Wiley & Sons, Inc.

on swelling and water transport in the HEMA network and also on the related optical properties.

The swelling behavior of crosslinked HEMA depends upon the balance of hydrophobic and hydrophilic interactions between polymer chains and water molecules.¹⁷ The balance of hydrophobic and hydrophilic forces in the polymer can be controlled by the addition of a crosslinking agent and hydrophobic monomers.^{13,18-21} The hydrophobic and hydrophilic components of polymer chains can also be modified by irradiation such as crosslink and scission. A radiation-induced reaction in an oxygen atmosphere or in air is significantly different from that in an inert atmosphere or in a vacuum.^{22,23} Oxygen reacts with radicals to form peroxide or hydroperoxide so that it prevents the recombination of the radical chain or crosslinking.^{24,25} The oxygen leads to an increase in the rate of scission process and degradation of the linear polymer such as poly(tetrafluoroethylene), poly(vinyl chloride), polypropylene, poly(acrylic acid), and so forth.^{24,25} During irradiation of polypropylene and poly(acrylic acid), scission occurs in an oxygen atmosphere whereas crosslinking occurs in a vacuum.^{24,25} However, the rate of chain scission in poly(methyl methacrylate) is lower in air than in a vacuum,²⁶ which is opposite to the above studies.^{23,24} With the energy of γ rays absorbed by polymers it is possible to form free radicals and unsaturated double bonds, which are the so-called color centers.^{24,27,28} The color center could change the optical properties of the polymer. All these issues are important in the application of HEMA, especially in the use of HEMA as contact lens materials. These issues prompted us to investigate the effect of γ -ray irradiation on water transport in HEMA copolymer with the presence of oxygen and the related phenomena.

Alfrey et al.²⁹ categorized the mass transport in the polymer as case I (concentration-gradient controlled), case II (stress-relaxation controlled), and anomalous diffusion (mixed case I with case II). The solutions of case I diffusion with different boundary conditions were collected by Crank.³⁰ The theory of case II diffusion was studied by Thomas and Windle,³¹ Govindjee and Simo,³² and Hui and Wu.^{33,34} The theoretical model of anomalous diffusion, which is a combination of case I and case II diffusion, was proposed by Wang et al.³⁵⁻³⁹ to analyze the semiinfinite specimen and modified by Harmon et al.^{40,41} to analyze a specimen of finite size. We use this combined model for our water transport analysis in this report.

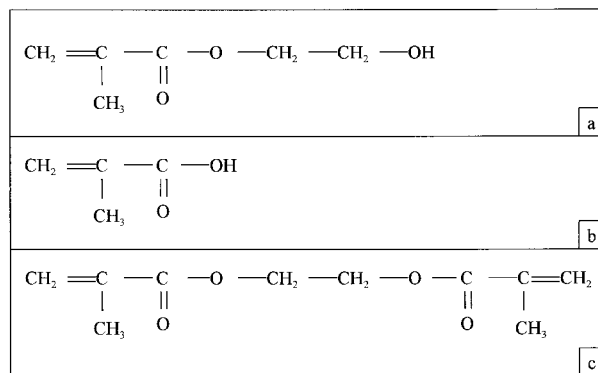


Figure 1. The chemical structure of (a) HEMA, (b) MAA, and (c) EDGMA.

We describe the experimental procedure. This is followed by the description of the determination of pH values of water used to immerse the irradiated HEMA copolymer and the water structure in the irradiated HEMA hydrogel that reveals the influence of the damage induced by irradiation on the HEMA samples. The radiation effect on the optical properties of the HEMA copolymer is also studied. A summary of findings obtained in this investigation is presented.

EXPERIMENTAL

The HEMA copolymer soft contact lens blanks were obtained from Canadian Contact Lens Laboratories Ltd. (Montreal, Canada). The compositions of HEMA copolymer consisted of HEMA, ethylene glycol dimethacrylate (EGDMA), and methacrylic acid (MAA); the chemical structures are listed in Figure 1. This copolymer contains the hydroxyl group, which is hydrophilic, the methyl group, which supports the hydrolytic stability, and the carboxyl group, which is highly ionizable. They were a standard 12.8-mm diameter and 6.0-mm thickness. These blanks were mounted on a bench lathe and thinned to 1.5 mm. The specimens were ground on 600 and 1200 grit emery papers and then polished with 1.0- and 0.05- μ m aluminum slurries. The final thickness was 1.44 mm. They were annealed for 1 week in a vacuum chamber at 60 °C and furnace cooled to 25 °C. The purpose of annealing was to release residual stresses in the specimen induced by machining.

In addition to the standard sample, which is the sample not subjected to γ -ray irradiation, the specimens were irradiated in air at 25 °C by a

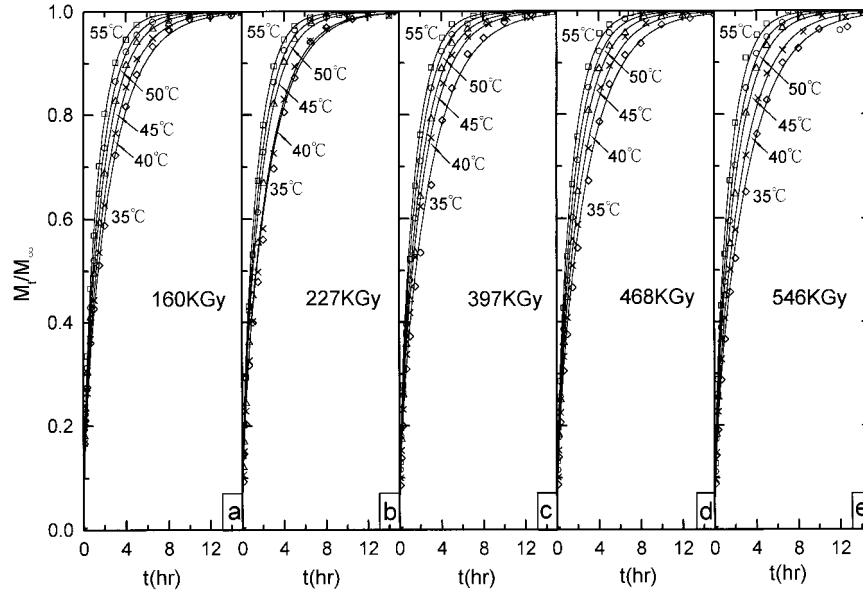


Figure 2. The water sorption in HEMA copolymer irradiated by γ rays in air: $\phi =$ (a) 0, (b) 160, (c) 227, (d) 397, (d) 468, and (e) 546 kGy.

30,000 Ci cobalt-60 source (Isotope Center of National Tsing Hua University) at the dosage rate of 7.1 kGy/h. The specimens were exposed for different periods to reach dosages of 160, 227, 397, 468, and 546 kGy.

For the absorption study the specimen was preweighed, preheated to the elevated temperature of the water transport study, and immersed in a deionized water filled glass bottle in a thermostatted water bath at the same temperature. The specimen was taken out periodically for measurements. Its surfaces were blotted and its mass was measured using an Ohaus Analytical Plus digital balance. After weighing the specimen was immediately returned to the water bath until the next measurement. The pH measurement of the solvent was conducted using a Jenco Electronics digital pH meter at 25 °C after the absorption experiment. The residue that leached out of the HEMA copolymer 400-kGy irradiated specimen into the water was analyzed using a Bruker DMX-600 NMR spectrometer.

The irradiated specimens were also cut into pieces of 2.5–3.5 mg and then immersed into deionized water at 40 °C until saturation. Each water-saturated specimen was enclosed in an aluminum pan and moved into a Seiko SSC II-5200H differential scanning calorimeter (DSC) for measurement. The temperature was increased from 25 to 100 °C with a heating rate of 5 °C/min and a nitrogen flow of 40 mL/min. For the study of the

water structure, the specimens immersed in water for different periods at 35–55 °C were cooled from 25 to –40 °C with a cooling rate of 5 °C/min, held at –40 °C for 20 min, and then heated from –40 to 30 °C with a heating rate of 5 °C/min. The heat flow of the system was recorded.

For the transmittance study the irradiated specimens were immersed in deionized water at different temperatures until saturation. All specimens were dehydrated in air at 25 °C. The transmittance was measured using a Hitachi U-3210/U-3240 Spectrometer ranging from 240 to 800 nm in air.

The surface morphology of irradiated specimens treated with water was observed using an Olympus BH-2 optical microscope.

RESULTS

Water Transport: Effect of γ -Ray Irradiation

Considering that the irradiated HEMA copolymer with half of the thickness l is immersed in deionized water, the data for deionized water transport in the irradiated HEMA copolymer at 35–55 °C are shown in Figure 2. These data can be analyzed by a mass transport model proposed by Harmon et al.^{40,41} Their model, which accounts for case I, case II, and anomalous transport, was successfully applied to several solvent–polymer

systems.^{42–44} In our case the water transport in irradiated HEMA copolymer can also be successfully analyzed by Harmon et al.'s model as shown below. This means that the water transport in the HEMA copolymer is anomalous transport behavior, which is a mixture of case I and case II transport and is controlled by both the chemical potential gradient and stress relaxation. From the curve fitting the characteristic parameters D and v corresponding to the diffusion coefficient of case I and the velocity of case II, respectively, can be obtained. The HEMA copolymer is initially assumed to be free of water, and the concentration of water is maintained constant on both outer surfaces at all times. The weight gain of water uptake, M_t , based on the 1-dimensional model is⁴⁰

$$\frac{M_t}{M_\infty} = 1 - 2 \sum_{n=1}^{\infty} \frac{\lambda_n^2 \left(1 - 2 \cos \lambda_n \exp\left(-\frac{vl}{2D}\right) \right)}{\beta_n^4 \left(1 - \frac{2D}{vl} \cos^2 \lambda_n \right)} \times \exp\left(-\frac{\beta_n^2 Dt}{l^2}\right) \quad (1)$$

where

$$\beta_n^2 = \frac{v^2 l^2}{4D^2} + \lambda_n^2 \quad (2)$$

and λ_n is the n th root of the following equation:

$$\lambda_n = \frac{vl}{2D} \tan \lambda_n. \quad (3)$$

The M_∞ is the final equilibrium–swelling ratio of water. The roots of eq. (3) (λ_n with $n = 1, 2, 3, \dots$) were used in eqs. (1) and (2). The solid lines in Figure 2 were plotted using eq. (1). We found that the theoretical model is in excellent agreement with the experimental data. The values of D and v obtained from Figure 2 are plotted in Figure 3(a,b), respectively. The D and v both increase with increasing temperature for a given dosage (ϕ) and decrease with an increasing dosage for a given temperature. The water transport based on case I and case II move from the outer surface to the center. The D and v both satisfy the Arrhenius equation and their activation energies were calculated and are tabulated in Table I. The activation energy of case I is increased with increasing dosage, but the trend for case II is in an opposite

direction. Case I diffusion is controlled by the chemical potential gradient, and case II transport is due to the stress relaxation of polymer chains. The above two mechanisms are influenced by the destruction of chemical bonds, crosslinks, and scission induced by irradiation.

The equilibrium–swelling ratio of water, S , is determined by the weight ratio of saturated water to the dry polymer. The data of S at different temperatures with various dosages are plotted in Figure 3(c). For a given dosage the value of S decreases with increasing temperature. The equilibrium–swelling ratios are curve fitted by the van't Hoff equation, $S = S_0 \exp(-\Delta H/RT)$, where S_0 , ΔH , R , and T are the preexponent factor, heat of mixing, gas constant, and temperature (K), respectively. The heats of mixing obtained for different dosages from Figure 3(c) are listed in Table I. The negative sign of the heat of mixing indicates that the mass transport is an exothermic process. The heat of mixing increases to a maximum at $\phi = 160$ kGy and then decreases with increasing dosage. For a given temperature, the value of S decreases with increasing dosage.

pH Value

The pH value was measured of the solvent with residual impurities leached out from the HEMA sample after mass transport at different temperatures. These data are tabulated in Table II. The pH value of deionized water at 25 °C is 6.1. For the standard HEMA sample, the water-induced hydrolysis of an ionizable carboxyl group and acidic products of the polymer are dissolved back into the solvent so that the pH value of the solvent after the mass transport experiment is lowered. The pH value decreases with increasing temperature. Because the concentration of the hydrogen ion is proportional to the exponential value of the negative pH value, the hydrogen ion concentration can be easily obtained from the pH values. The hydrogen ion increment is determined by the ratio of the difference of H^+ concentrations after and before the mass transport experiment to the H^+ concentration in the solvent before the mass transport experiment. The curve of the logarithmic hydrogen ion increment ($\Delta[H^+]$) in the solvent versus the reciprocal of the mass transport temperature is plotted in Figure 4. The reaction heat obtained from the slope is equal to 19.657 kcal/mol. The hydrolysis process is endothermic for the standard specimen. The pH value of the solvent immersed with the irradiated

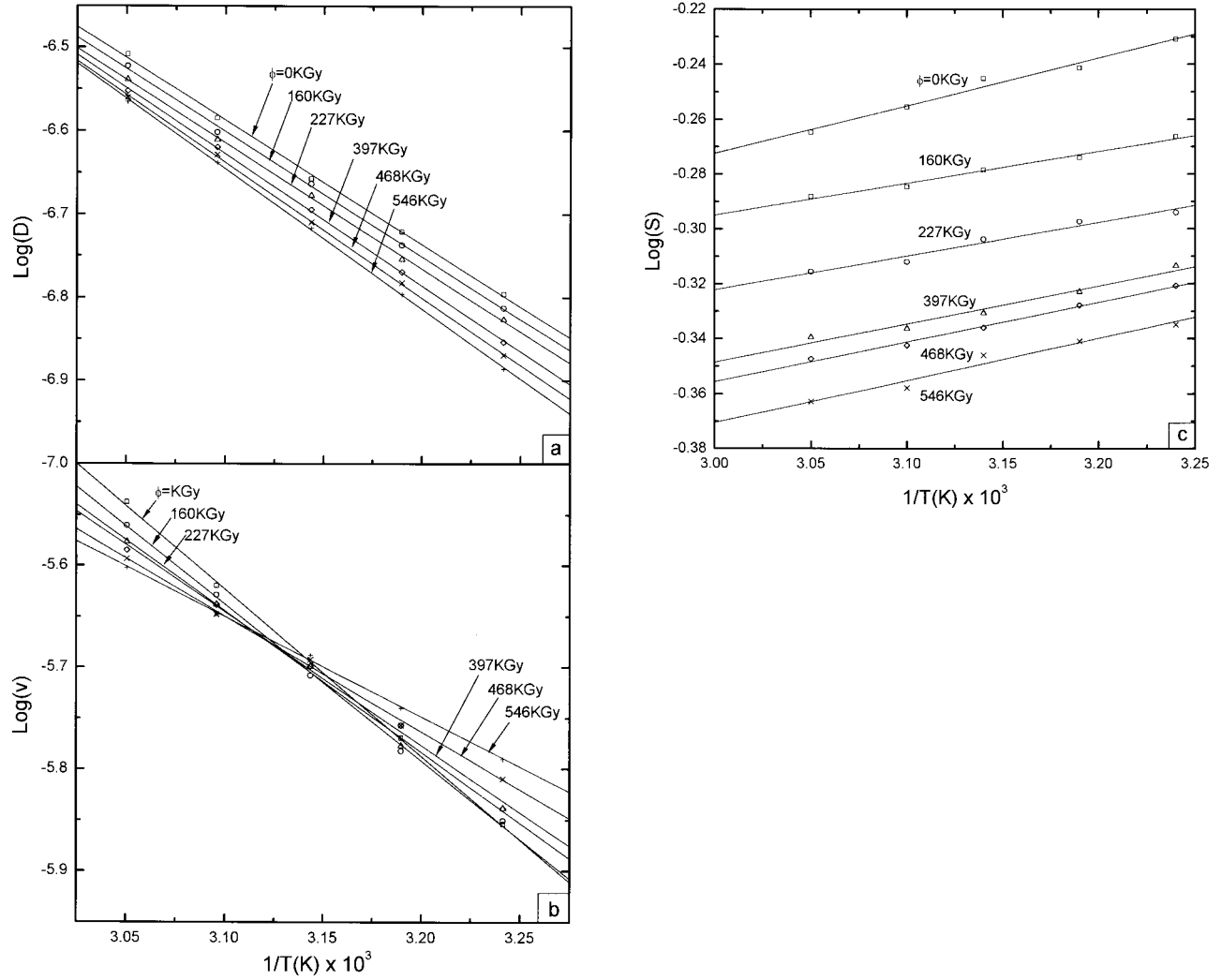


Figure 3. Arrhenius plots of (a) the diffusion coefficient, D , for case I, (b) velocity, v , for case II, and (c) the van't Hoff plot of the equilibrium-swelling ratio, S , for different dosages.

specimen is lower than that immersed with the standard specimen. This implies that some bond breakage happened during irradiation, which caused the formation and leaching of the acid group into the solvent. On the other hand, for a given irradiation dosage, the pH value does not increase with decreasing temperature. The max-

imum pH value is at 50 °C for $\phi = 160$ kGy and 45 °C for $\phi \geq 227$ kGy. At higher temperatures the hydrolysis is more active whereas at lower temperatures the hydrolysis reaction probability is raised because of the higher water content in the hydrogel. Both cases are favorable to acidify the solvent and give a probable explanation of the

Table I. Activation Energies of Case I, E_D , and Case II, E_v , and Heat of Mixing ΔH

ϕ (kGy)	0	160	227	397	468	546
E_D (kcal/mol)	6.84 ± 0.15	6.87 ± 0.12	6.92 ± 0.13	7.24 ± 0.06	7.43 ± 0.16	7.69 ± 0.08
E_v (kcal/mol)	7.53 ± 0.13	7.06 ± 0.14	6.37 ± 0.15	6.03 ± 0.16	5.21 ± 0.11	4.51 ± 0.15
ΔH (kcal/mol)	-0.79 ± 0.06	-0.52 ± 0.03	-0.56 ± 0.05	-0.63 ± 0.03	-0.66 ± 0.02	-0.70 ± 0.05

Table II. pH Values of Deionized Water after Immersion of HEMA Copolymer at 25 °C

Mass Transport Temp. (K)	ϕ (kGy)					
	0	160	227	397	468	546
328	5.23 ± 0.01	4.41 ± 0.02	4.44 ± 0.03	4.17 ± 0.04	4.14 ± 0.01	4.08 ± 0.02
323	5.41 ± 0.02	4.43 ± 0.03	4.51 ± 0.03	4.28 ± 0.02	4.25 ± 0.03	4.18 ± 0.03
318	5.60 ± 0.01	4.36 ± 0.01	4.56 ± 0.01	4.32 ± 0.02	4.30 ± 0.02	4.27 ± 0.01
313	5.71 ± 0.02	4.25 ± 0.02	4.50 ± 0.02	4.30 ± 0.03	4.26 ± 0.01	4.20 ± 0.02
308	5.82 ± 0.01	4.10 ± 0.01	4.47 ± 0.03	4.20 ± 0.01	4.14 ± 0.03	4.10 ± 0.04

maximum pH value at an intermediate temperature.

The NMR study of the residues in water provides evidence of the formation of acidic group. The ^1H NMR spectra of residues of the 400-kGy HEMA copolymer in water are shown in Figure 5. According to the NMR spectrum handbook of organic chemicals,⁴⁵ the compositions of the residues are ethanol and ethylene glycol. The bond between oxygen and the ethyl group in the side chains of HEMA and EGDMA were broken by γ rays, so that the carboxyl group appeared and acidified the water-HEMA copolymer system. Based on the above analysis, some of the hydrophilic side chains of the HEMA copolymer were destroyed by γ -ray irradiation, so the equilibrium-swelling ratio of the irradiated specimen was lowered.

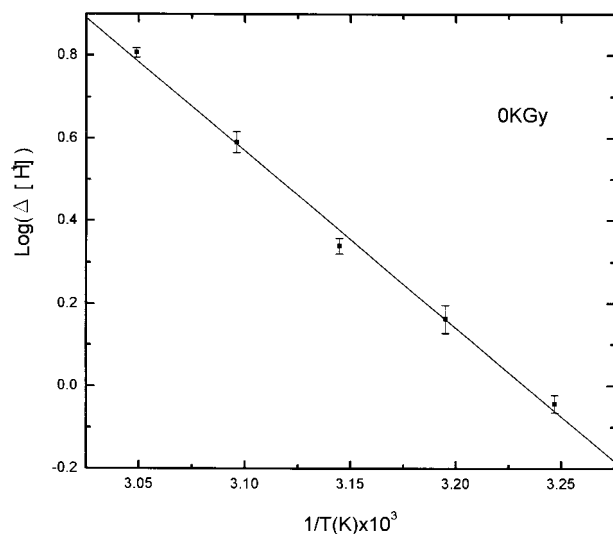


Figure 4. The plot of the logarithmic hydrogen ion increment ($\Delta[\text{H}^+]$) in the deionized water after immersion of HEMA copolymer versus the reciprocal of mass transport temperature.

Thermal Analysis

The glass transition temperature of the irradiated HEMA copolymer with dosages less than 546 kGy is maintained at 327 K before being immersed in water. This implies that the effect of a sole γ ray on the glass transition temperature is insignificant. However, after water saturation the glass transition temperatures of dry specimens (after dehydration) irradiated by γ rays with a dosage range of 0–546 kGy were changed from 289 to 284 K. This implies that the chain scission affected by the γ ray on the copolymer is slightly greater than the crosslinking. However, the effect on the glass transition point became apparent only when the detached chains were dissolved in the solvent, and the HEMA network was dehydrated and dried again. This implies that the local chain configuration is statistically different from that before the irradiation-hydration-dehydration process, resulting in different glass transition temperatures.

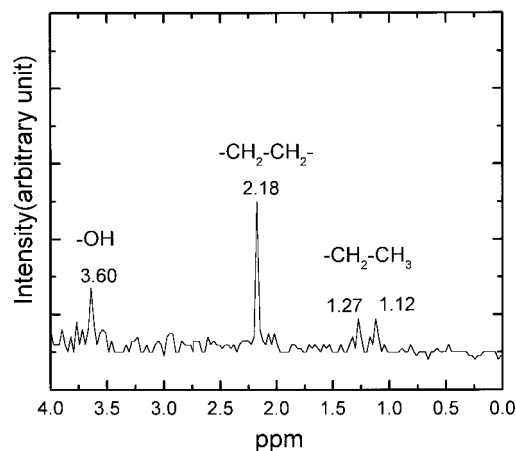


Figure 5. The ^1H NMR spectra of the residues of HEMA copolymer irradiated with 400 kGy in 50 °C water.

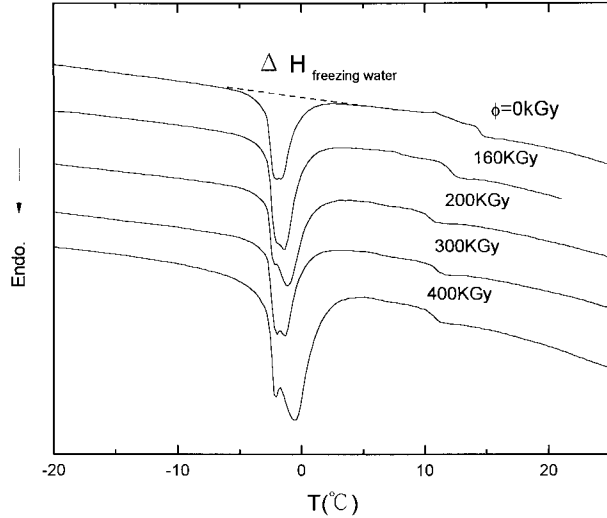


Figure 6. The endotherms of water-HEMA hydrogels with different dosages.

A further investigation of the effect of irradiation on polymer chains was made by the DSC analysis of the water structure in the hydrogel. The water structure in the hydrogel is generally categorized as the nonfreezing (bound) water and the freezing (free) water.^{21,46–48} This means that the total content of water S_t is the summation of the contents of the freezing water S_f and the nonfreezing water S_{nf} :

$$S_t = S_f + S_{nf}. \quad (4)$$

The molecule of nonfreezing water is hydrogen bonded to the hydrophilic groups: the content of nonfreezing water is proportional to the amount of hydrophilic groups in the polymer. On the other hand, the freezing water is in a state of pure water independent of the polymeric structure. The content of freezing water is affected by the chain mobility or crosslink density of the polymer.^{13,14} Thus, the determination of two types of water in the hydrogel is helpful to understand the crosslink and scission effect or the destruction of the hydrophilic group induced by γ rays. During the heating process of the DSC analysis, an endothermic melting peak appeared in the freezing water at 0 °C, but not in the nonfreezing water. Thus, both types of water in the hydrogel can be determined by the DSC analysis.^{12–14,49} The endothermic melting peaks of freezing water at 0 °C for the saturated hydrogel are shown in Figure 6. The peak area covered for the melting of freezing water is calculated ($\Delta H_{\text{freezing water}}$), then the con-

tent of freezing water (S_f) can be obtained by the following equation⁴⁹:

$$S_f = \frac{W_{\text{freezing water}}}{W_{\text{polymer}}}, \quad (5)$$

where $W_{\text{freezing water}}$ and W_{polymer} are the weights of freezing water and dry polymer, respectively, and

$$W_{\text{freezing water}} = \frac{\Delta H_{\text{freezing water}}}{\Delta h_{\text{em}}}. \quad (6)$$

In eq. (6) the $\Delta H_{\text{freezing water}}$ is the enthalpy in the reaction and Δh_{em} is the effective specific fusion heat of water in the hydrogel.^{49–51} Substituting eqs. (6) and (4) into eq. (5) one can obtain

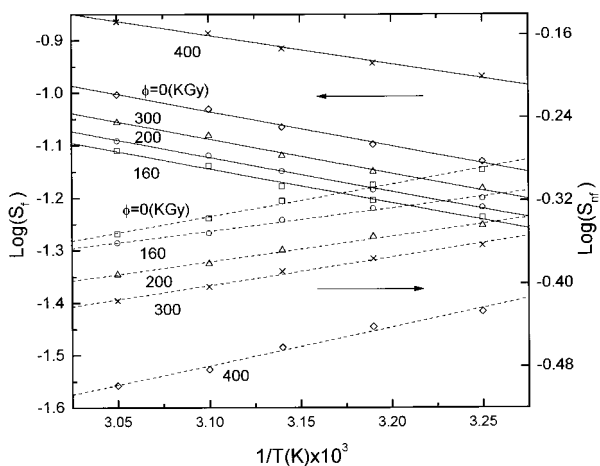
$$S_f = S_t - S_{nf} = \frac{\Delta H_{\text{freezing water}}}{\Delta h_{\text{em}} W_{\text{polymer}}} \quad (7)$$

At a given temperature the value of S_{nf} in the hydrogel with various S_t is fixed. Thus, from eq. (7) the relationship between S_t and $\Delta H_{\text{freezing water}}$ is linear. The Δh_{em} and S_{nf} can be obtained from the linear regression of eq. (7). The data of the DSC analysis are listed in Table III. For a given dosage, the content of freezing water follows the van't Hoff equation as shown in Figure 7 and the transport process is endothermic. From Figure 7 we also obtain the heat of mixing for various dosages, and the data are tabulated in Table III. The heat of mixing for freezing water is maintained at 2.98 ± 0.05 kcal/mol below $\phi = 300$ kGy and then decreases to 2.49 kcal/mol for $\phi = 400$ kGy. This implies that more network chains are destroyed for $\phi = 400$ kGy than for $\phi \leq 300$ kGy. For a given temperature the content of freezing water in the hydrogel has a minimum at $\phi = 160$ kGy and then increases with increasing dosage. This also implies that more crosslinks are induced than the network chains that are destroyed with a low dosage of irradiation and vice versa with a high irradiation dosage above the critical value (>300 kGy). On the other hand, the content of nonfreezing water also follows the van't Hoff equation as shown in Figure 7. The transport process of nonfreezing water is exothermic and its heat of mixing (ΔH_{nf}) has a minimum at $\phi = 160$ kGy. The change of ΔH_{nf} is related to the structural variation of side chains and acidification of the solvent-polymer system. The content of nonfreezing water decreases monotonically with in-

Table III. Water Contents of Freezing (S_f) and Nonfreezing Water (S_{nf}), Effective Specific Heat of Fusion of Water (Δh_{em}), and Heat of Mixing of Freezing (ΔH_f) and Nonfreezing Water (ΔH_{nf}) in Hydrogel for HEMA Copolymer

ϕ (kGy)	T (K)	S_{nf} (wt %)	S_f (wt %)	Δh_{em} (J/g)	ΔH_{nf} (kcal/mol)	ΔH_f (kcal/mol)
0	328	44.43 ± 0.51	9.93 ± 0.20	282	-1.44 ± 0.08	3.01 ± 0.13
	323	46.02 ± 0.53	9.32 ± 0.19	285		
	318	47.84 ± 0.71	8.61 ± 0.13	287		
	313	49.54 ± 0.68	7.97 ± 0.14	290		
	308	51.20 ± 0.59	7.40 ± 0.16	292		
160	328	43.55 ± 0.49	7.76 ± 0.22	280	-1.02 ± 0.05	2.98 ± 0.09
	323	44.52 ± 0.35	7.26 ± 0.18	283		
	318	45.87 ± 0.53	6.63 ± 0.17	284		
	313	47.03 ± 0.45	6.24 ± 0.20	282		
	308	48.11 ± 0.42	5.78 ± 0.21	281		
200	328	40.60 ± 0.44	8.10 ± 0.21	279	-1.12 ± 0.06	2.99 ± 0.10
	323	41.63 ± 0.51	7.61 ± 0.16	281		
	318	42.86 ± 0.38	7.09 ± 0.18	282		
	313	44.15 ± 0.41	6.53 ± 0.13	281		
	308	45.28 ± 0.48	6.04 ± 0.15	279		
300	328	38.32 ± 0.50	8.78 ± 0.18	277	-1.24 ± 0.07	2.99 ± 0.11
	323	39.55 ± 0.37	8.29 ± 0.20	280		
	318	40.91 ± 0.46	7.59 ± 0.17	281		
	313	42.08 ± 0.42	7.08 ± 0.14	279		
	308	43.34 ± 0.35	6.56 ± 0.19	278		
400	328	35.81 ± 0.48	9.59 ± 0.19	273	-1.71 ± 0.06	2.49 ± 0.10
	323	36.73 ± 0.46	9.18 ± 0.20	274		
	318	37.98 ± 0.53	8.72 ± 0.14	277		
	313	39.12 ± 0.50	8.42 ± 0.16	276		
	308	40.25 ± 0.41	7.90 ± 0.17	274		

creasing dosage. The reduction of nonfreezing water is equivalent to the loss of hydrophilic groups due to the γ -ray irradiation.

**Figure 7.** The van't Hoff plots of the equilibrium-swelling ratio of the freezing water (S_f) and nonfreezing water (S_{nf}) for different dosages.

In summary, the crosslinks induced by γ rays are dominant at a low irradiation dosage, for which the scission is significant at high dosage, and the destruction of hydrophilic groups occurs at all doses. The water absorbed in the hydrogel can be differentiated by the freezing and nonfreezing water. The ΔH_{nf} has a minimum at $\phi = 160$ kGy, as does the heat of mixing, ΔH .

Change of Optical Property

The transmittance, I , of specimens with various dosages before and after the water uptake as a function of wavelength, λ , is plotted in Figure 8(a,b), respectively. In the range of the visible spectrum (400–800 nm) we found that the transmittance of the standard specimen after water treatment was lower than that before water treatment. The penetration of water enlarges the spaces between the polymer chains. The polymer chains cannot recover completely after desorption, so some holes (or voids) remain in the HEMA

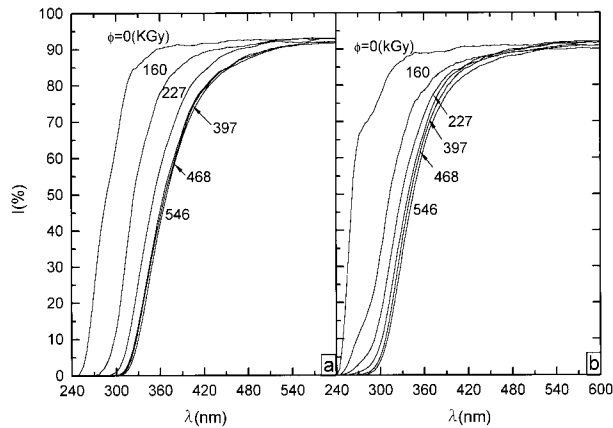


Figure 8. The transmission spectrum of standard and irradiated HEMA copolymers (a) before water absorption and (b) after water saturation at 50 °C.

copolymer as shown in Figure 9. These holes induce light scattering. As a result, the transmittance of the standard specimen is lowered after water treatment. For irradiated HEMA copolymer, color centers are created in the specimen by the γ -ray irradiation so that the light of the shorter wavelength is absorbed, as shown in Figure 8(a). However, these color centers are annihilated by hydrolysis. The elimination of these obstacles generated by irradiation in the optical path is more pronounced than the creation of holes after dehydration. Because the thermal stability of the irradiated samples is lowered after the water treatment, the observation of holes in the specimens by SEM was difficult. Therefore, the transmittance of irradiated HEMA copolymers after desorption is raised, as shown in Figure 8(b). In the range of the near UV (240–400 nm) spectrum, we also found that light with a wavelength below 250 nm was completely absorbed in the standard specimen. The maximum absorbed wavelength is called the cutoff wavelength. The cutoff wavelengths of the HEMA copolymer before water treatment were 250, 270, 288, 299, 302, and 305 nm for $\phi = 0, 160, 227, 397, 468,$ and 546 kGy, respectively. The cutoff wavelength of the copolymer increased with increasing dosage. It results from the unstable factors such as free radicals,⁵² peroxides, hydroperoxides, and other oxygen-containing species produced by the reaction of radicals and oxygen,^{53,54} which absorbs light in this region.⁵⁵ The cutoff wavelengths of HEMA copolymer after water treatment were 240, 245, 248, 258, 270, and 279 nm for $\phi = 0, 160, 227, 397, 468,$ and 546 kGy, respectively. For the same dosage the cutoff wave-

length was smaller for the postwater treatment than for the prewater treatment. This was because of the dissolution of chromophores (such as a carbonyl group) or auxochromes (such as an hydroxyl group) in the copolymers into water and the disappearance of some unstable factors resulting from hydration.

Buckled Pattern on Surface

The surface morphology of HEMA copolymers irradiated with 200 kGy before immersion in water is shown in Figure 10(a). The surface is smooth with no pattern observed. When this specimen was immersed in water for 5 min, the surface showed a buckled pattern [Fig. 10(b)]. The size of the pattern increased monotonically with increasing immersion time as shown in Figure 10(c–g). The buckled pattern can be analyzed using the 2-dimensional Fourier transform. Figure 11 shows the Fourier-transformed profiles in the q space corresponding to Figure 10(g) (in the real space). It can be seen from Figure 11 that an isotropic ring pattern indicates that there is no preferred orientation. As a result, the curve of radial average intensity versus q reveals several peaks. Figure 12 shows the radial average intensity, A , as a function of q and immersion time where the unit of A is the intensity index shown in Figure 11. Neglecting the intensity in the neighborhood of $q = 0$, the first and second maximum intensities increased to a maximum and then decreased with increasing immersion time. The q values corresponding to the first and second maximum intensities decrease monotonically

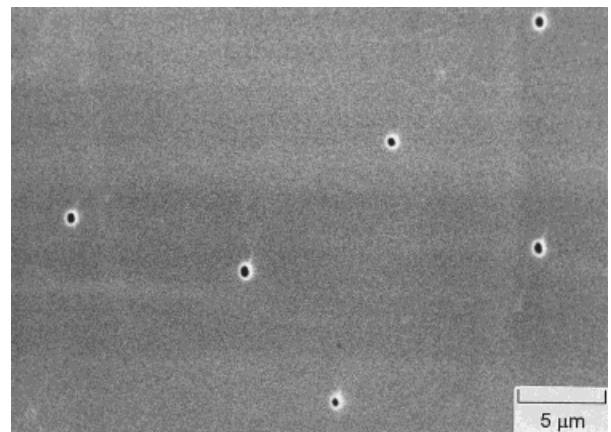


Figure 9. The cross section of the standard HEMA copolymer as observed by SEM after being saturated with water and then desorbed.

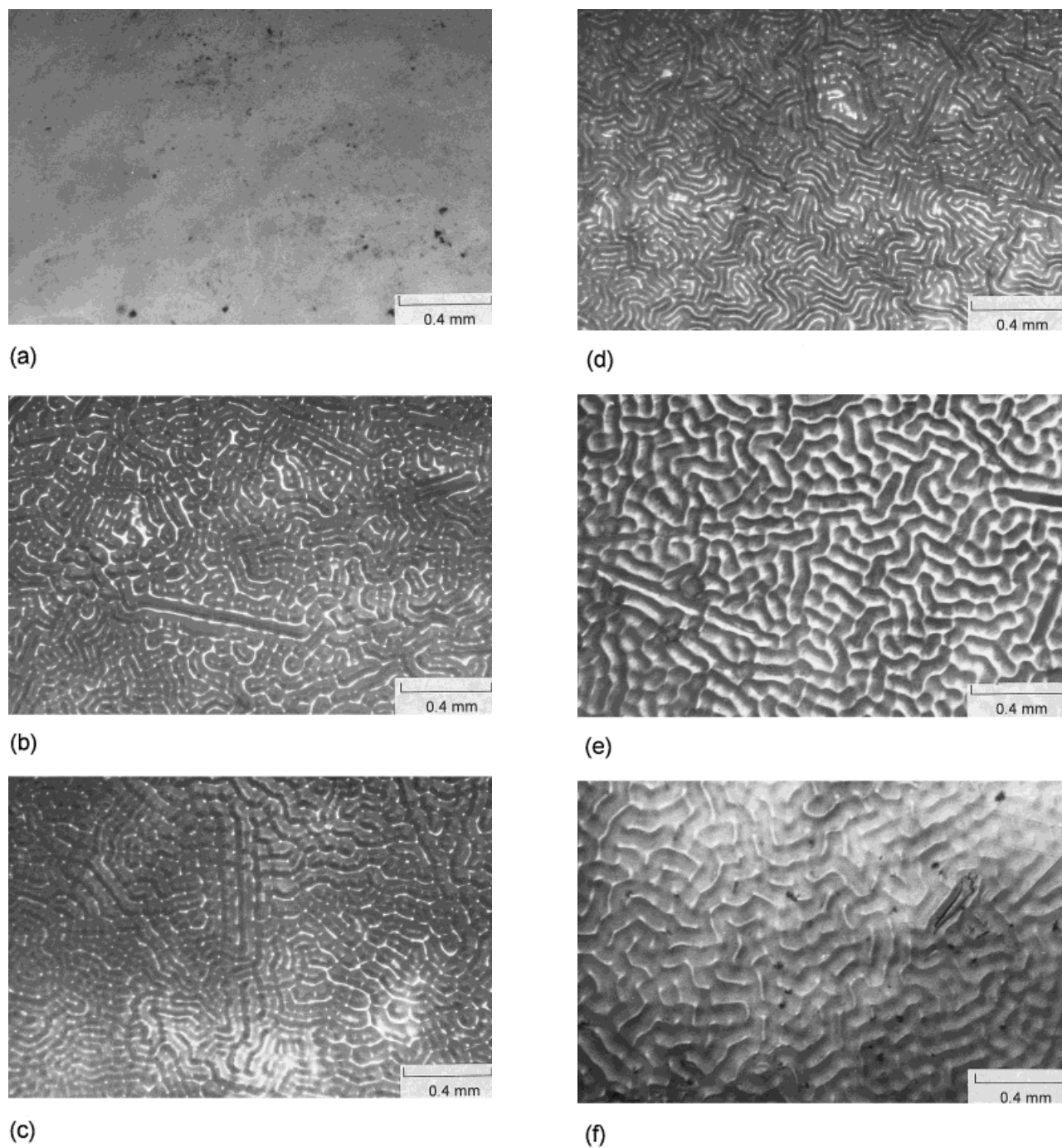
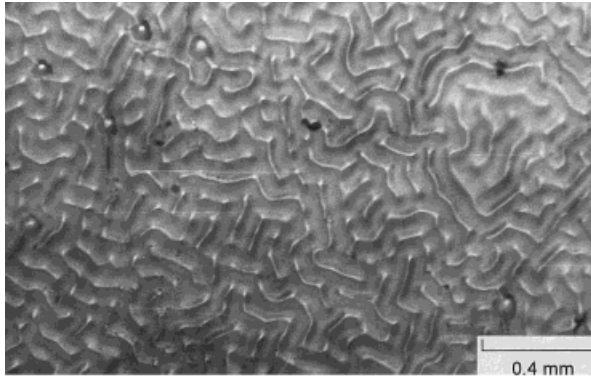


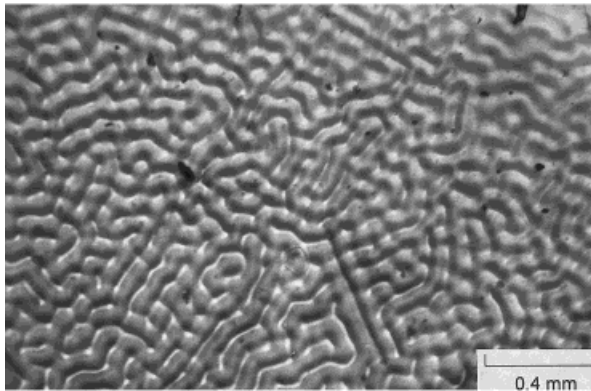
Figure 10. The buckled pattern on the surface of the irradiated (200 kGy) HEMA copolymer immersed in water at 50 °C that was observed with an optical microscope for (a) 0, (b) 5, (c) 20, (d) 60, (e) 180, (f) 360, and (g) 630 min; (h) desorption in air for 1 month; and (i) the cross section of HEMA copolymer saturated in water at 40 °C.

with increasing immersion time. Because the q space is the reciprocal space of the buckled pattern, this is an alternative and convenient way to examine the averaged size and amplitude of the buckled pattern instead of carrying out a compli-

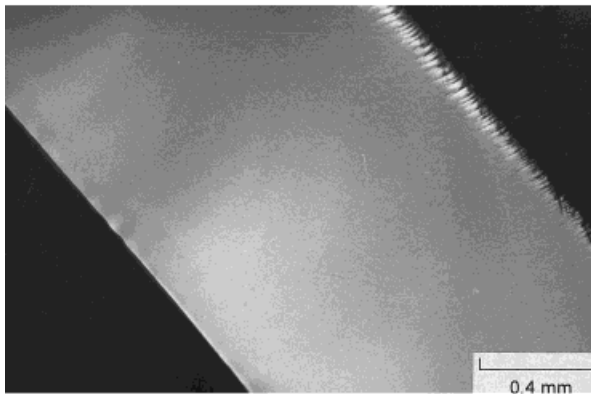
cated image analysis in the real space. From this q -space analysis it is obvious that the buckled size increases with increasing immersion time. When water is desorbed from the specimen, the buckled pattern still exists but its size is reduced as shown



(g)



(h)



(i)

Figure 10. (Continued from the previous page)

in Figure 10(h). This phenomenon disappears in the specimen with a higher dosage of irradiation and a longer time of immersion. The buckled pattern is observed in the specimen irradiated by γ rays in the air atmosphere but not in a vacuum. The morphology of the cross section of the HEMA copolymer irradiated by γ rays in air and saturated with water at 40 °C is shown in Figure 10(i).

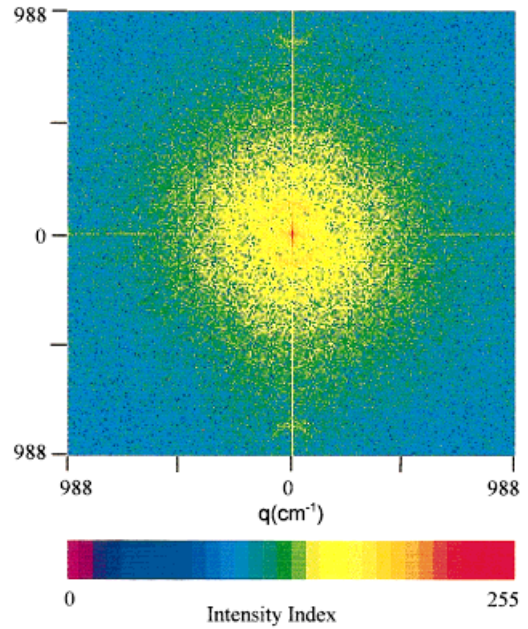


Figure 11. The Fourier transformed profiles in q space corresponding to Figure 10(g) for the immersion time 630 min.

We found that the saw-tooth shape appearing on the upper right region corresponds to the buckled pattern and the other regions are smooth. This evidence shows that the buckled pattern appears on the surface facing the air not in the bulk region. A similar pattern was found in polyvinyl gels by Tanaka et al.^{56,57} They proposed that the occurrence of the buckled pattern resulted from the mechanical instability between the swollen outer layer and the fixed inner layer in the pro-

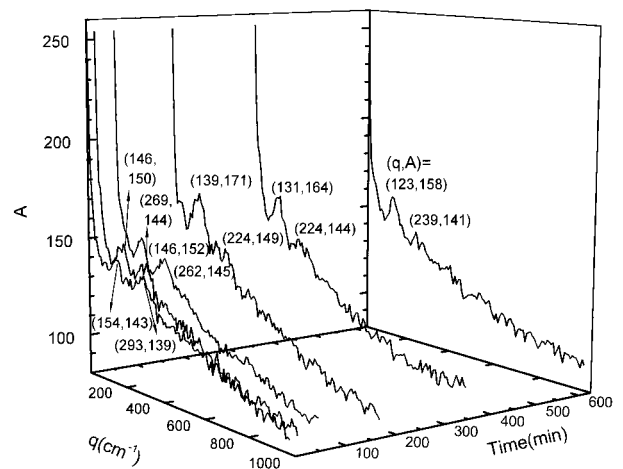


Figure 12. The radial average intensity, A , as a function of q and immersion time.

cess of collective diffusion. In this study the pattern only appeared on the irradiated specimen, but the surface of the standard specimen remained smooth throughout the entire mass transport process. The swelling in the outer layer of the specimen irradiated in air was significantly different from that in the bulk region. This was probably created by the inhomogeneous crosslinking and chain scission in this surface region.

The buckled pattern was not observed on the surface of HEMA copolymer irradiated by γ rays in a vacuum immersed in water; it was only on those irradiated in the air. This is consistent with the explanation that oxygen is present and also diffuses into the HEMA copolymer from the outer surface when the specimen is irradiated in air. Oxygen will react with radicals and prevent the radical recombination to form crosslinking. The crosslinking density increases with increasing depth from the outer surface. During the water uptake the outer surface was swollen first, which is similar to that observed by Tanaka et al.^{56,57} This inhomogeneous swollen condition was identified as the cause by the mechanical instability of the buckled pattern. The size of the buckled pattern depends on the swelling condition and profile during water uptake. As seen in Figure 10(h), the buckled pattern still exists after desorption at 200 kGy. It is an indication that the outer surface still remains at a higher swollen state than the inner region. On the other hand, for the case of high dosages, the chain scission really dominates. The crosslinking density at the outer surface is either too low or the difference in crosslinking densities (inhomogeneity) is insignificant to maintain the buckled pattern on the outer surface. Therefore, the final pattern appears very smooth for a HEMA copolymer with high dosage irradiation and immersed in water for a long time.

SUMMARY

The water transport in HEMA copolymer irradiated by γ rays in an air atmosphere and associated phenomena are investigated. The water uptake data are in excellent agreement with the theoretical model for all irradiated dosages: the water transport behavior is an anomalous transport and the diffusion coefficient of case I and the velocity of case II are obtained from curve fitting. The diffusion coefficient and the velocity characterized for cases I and II diffusion both satisfy the Arrhenius equation. The activation energy of case

I increases gradually with an increasing amount of dosage, but the trend of activation energy of case II is the opposite. The equilibrium–swelling ratio satisfies the van't Hoff plot and the mass transfer is an exothermic process. The heat of mixing increases monotonically with increasing dosage in the range of 160–546 kGy and is lower than that of the standard (unirradiated) specimen.

The decrease of pH values of the solvent after the mass transport and the determination of residues in water by NMR show the loss of the hydrophilic group from the network. The freezing and nonfreezing water are analyzed by the endothermic melting peak from the DSC measurement. Freezing and nonfreezing water contents in the hydrogel decrease with increasing dosage, but the trend of freezing water content is opposite at high dosages. This implies that the crosslinking and scission processes are dominant at low and high dosages, respectively. The decrease of nonfreezing water content is other evidence of the destruction of the hydrophilic group. The freezing and nonfreezing water both satisfy the van't Hoff plot. The former is endothermic and the latter is exothermic. The heat of mixing for nonfreezing water has a minimum at $\phi = 160$ kGy.

The cutoff wavelength of the HEMA copolymer before and after water treatment at 55 °C increases with increasing dosage. It is smaller for postwater treatment than for the prewater treatment. The buckled pattern appears on the outer surface of the HEMA copolymer irradiated with 200 kGy in air and treated with water. The size of the buckled pattern increases monotonically with increasing immersion time until it reaches the equilibrium. This can be analyzed by 2-dimensional Fourier transform (in q space). The q values corresponding to the first two maximum intensities decrease with increasing immersion time. This is consistent with the idea that the size of the buckled pattern increases with increasing immersion time. A simple model based on the mechanical instability arising from the inhomogeneous distribution of crosslinking density is used to explain the formation of the buckled pattern.

This work was supported by the National Science Council, Taiwan, Republic of China.

REFERENCES AND NOTES

1. Refojo, M. F. *Encyclopedia of Polymer Science and Technology*; Wiley: New York, 1976; Supplement 1, p 195–219.

2. Wichterle, O.; Lim, D. *Nature* 1960, 185, 117.
3. Ratner, B. D.; Miller, I. F. *J Biomed Mater Res* 1973, 7, 353.
4. Vacik, J.; Czakova, M.; Exner, J.; Kopecek, J. *Collection Czechoslovak Chem Commun* 1977, 42, 2786.
5. Tollar, M.; Stol, M.; Kliment, K. *J Biomed Mater Res* 1969, 3, 305.
6. Lazarus, S. M.; LaGuerre, J. N.; Kay, H.; Weinberg, S. R.; Levowitz, B. S. *J Biomed Mater Res* 1971, 5, 129.
7. Pedley, D. G.; Skelly, P. J.; Tighe, B. J. *Br Polym J* 1980, 12, 99.
8. Larke, J. R.; Tighe, B. J. (to National Research Development Corporation) *Br. Pat.* 1(395), 501, 1975.
9. Janacek, J. J. *Macromol Sci Rev Macromol Chem* 1973, 9, 1.
10. Refojo, M. F. *J Polym Sci A-1* 1967, 5, 3103.
11. Klotz, I.; Franzen, J. *J Am Chem Soc* 1962, 84, 3461.
12. Lee, H. B.; John, M. S.; Andrade, J. D. *J Colloid Interface Sci* 1975, 51, 225.
13. Sung, Y. K.; Gregonis, D. E.; John, M. S.; Andrade, J. D. *J Appl Polym Sci* 1981, 26, 3719.
14. Smyth, G.; Quinn, F. X.; McBrierty, V. J. *Macromolecules* 1988, 21, 3198.
15. Pathamanathan, K.; Johari, G. P. *J Polym Sci (B) Polym Phys* 1990, 28, 675.
16. Jeyanthi, R.; Rao, K. P. *J Appl Polym Sci* 1991, 43, 2333.
17. Refojo, M. F.; Yasuda, H. *J Appl Polym Sci* 1965, 9, 2425.
18. Corkhill, P. H.; Jolly, A. M.; Ng, C. O.; Tighe, B. J. *Polymer* 1987, 28, 1758.
19. Warren, T. C.; Prins, W. *Macromolecules* 1972, 5, 506.
20. Pedley, D. G.; Tighe, B. J. *Br Polym J* 1979, 11, 130.
21. Frommer, M. A.; Lancet, D. *J Appl Polym Sci* 1972, 16, 1295.
22. Kudoh, H.; Sasuga, T.; Seguchi, T.; In *Irradiation of Polymers: Fundamentals and Technological Applications*; Clough, R. L.; Shalaby, S., Eds.; American Chemical Society: Washington, D.C., 1996; pp 2-10.
23. Gupta, M. C.; Srivastava, A. K. *J Polym Sci Polym Chem Ed* 1982, 20, 541.
24. Gupta, M. C.; Deshmukh, V. G. *Polymer* 1983, 24, 827.
25. Mark, J. E. In *Physical Properties of Polymers Handbook, Part VIII*; American Institute of Physics: New York, 1996; p 561-562.
26. Wall, L. A.; Brown, D. W. *J Phys Chem* 1957, 61, 129.
27. Ohnishi, S.; Nakajima, Y.; Nitta, S. *J Appl Polym Sci* 1962, 5, 629.
28. Barker, R. E., Jr.; Moulton, W. G. *J Polym Sci* 1960, 47, 175.
29. Alfrey, T.; Gurnee, E. F.; Lloyd, W. G. *J Polym Sci (C)* 1966, 12, 249.
30. Crank, J. *The Mathematics of Diffusion*, 2nd ed.; Oxford University Press: Oxford, U.K., 1975.
31. Thomas, N. L.; Windle, A. H. *Polymer* 1982, 23, 529.
32. Govindjee, S.; Simo, J. C. *J Mech Phys Solids* 1993, 41, 863.
33. Hui, C.-Y.; Wu, C.-K. *J Appl Phys* 1987, 61, 5129.
34. Hui, C.-Y.; Wu, C.-K. *J Appl Phys* 1987, 61, 5137.
35. Wang, T. T.; Kwei, T. K.; Frisch, H. L. *J Polym Sci A-2* 1969, 7, 2019.
36. Kwei, T. K.; Wang, T. T.; Zupko, H. M. *Macromolecules* 1972, 5, 645.
37. Kwei, T. K.; Zupko, H. M. *J Polym Sci A-2* 1969, 7, 876.
38. Wang, T. T.; Kwei, T. K. *Macromolecules* 1973, 6, 919.
39. Frisch, H. L.; Wang, T. T.; Kwei, T. K. *J Polym Sci A-2* 1969, 7, 8.
40. Harmon, J. P.; Lee, S.; Li, J. C. M. *J Polym Sci Polym Chem Ed* 1987, 25, 3215.
41. Harmon, J. P.; Lee, S.; Li, J. C. M. *Polymer* 1988, 29, 1221.
42. Wu, T.; Lee, S.; Chen, W. C. *Macromolecules* 1995, 28, 5751.
43. Ouyang, H.; Lee, S. *J Mater Res* 1997, 12, 2794.
44. Ouyang, H.; Chen, C. C.; Lee, S.; Yang, H. J. *J Polym Sci (B) Polym Phys* 1998, 36, 163.
45. Grasselli, J. G.; Ritchey, W. M. *Atlas of Spectral Data and Physical Constants for Organic Compounds*; CRC Press: Cleveland, OH, 1975.
46. Froix, M.; Nelson, R. A. *Macromolecules* 1975, 8, 726.
47. Hatakeyama, T.; Yamauchi, A.; Hatakeyama, H. *Eur Polym J* 1984, 20, 61.
48. Krishnamurthy, S.; McIntyre, D.; Santee, E. R.; Wilson, C. W. *J Polym Sci Polym Phys Ed* 1973, 11, 427.
49. Ahmad, M. B.; O'Mahony, J. P.; Huglin, M. B.; Davis, T. P.; Ricciardone, A. G. *J Appl Polym Sci* 1995, 56, 397.
50. Pouchly, J.; Biroš, J.; Benes, S. *Makromol Chem* 1979, 180, 745.
51. Quinn, F. X.; Kampff, E.; Smyth, G.; McBrierty, V. J. *Macromolecules* 1988, 21, 3191.
52. Wall, L. A.; Florin, R. E. *J Appl Polym Sci* 1959, 2, 251.
53. Reichmanis, E.; Frank, C. W.; O'Donnell, J. H. *Irradiation of Polymeric Materials: Processes, Mechanisms, and Applications*; American Chemical Society: Washington, D.C., 1993; Chapter 1.
54. Harmon, J. P.; Biagtan, E.; Schueneman, G. T.; Goldberg, E. P. In *Irradiation of Polymers: Fundamentals and Technological Applications*; Clough, R. L.; Shalaby, S. W., Eds.; American Chemical Society: Washington, D.C., 1996; Chapter 23.
55. Bamford, C. H.; Jenkins, A. D.; Symons, M. C. R.; Townsend, M. G. *J Polym Sci* 1959, 34, 181.
56. Tanaka, T. *Phys Rev Lett* 1978, 40, 820.
57. Tanaka, T.; Sun, S. T.; Hirokawa, Y.; Katayama, S.; Kucera, J.; Hirose, Y.; Amiya, T. *Nature* 1987, 325, 796.